FABAD J. Pharm. Sci., 51, 3, 1249-1268, 2026
Doi: 10.55262/fabadeczacilik.2008904
RESEARCH ARTICLE

LC–MS-Based Untargeted Metabolomics Characterizes Caffeine-Associated Metabolic Remodeling in LPS-Stimulated RAW 264.7 Macrophages

Ozan KAPLAN[*°], Ahmet AVCI[**], Vahap Murat KUTLUAY[***]

LC–MS-Based Untargeted Metabolomics Characterizes Caffeine-Associated Metabolic Remodeling in LPS-Stimulated RAW 264.7 Macrophages

SUMMARY

Caffeine is a widely consumed methylxanthine with reported immunomodulatory properties, but its broader effects on inflammation-associated metabolic reprogramming remain incompletely characterized. In this study, we used LC–MS-based untargeted intracellular metabolomics to investigate caffeine-associated metabolic alterations in lipopolysaccharide (LPS)-stimulated RAW 264.7 macrophages. Cell viability analysis indicated that 0.2 mM caffeine maintained viability comparable to untreated control cells, and this concentration was selected for metabolomic analysis. Untargeted LC–QTOF–MS profiling (n = 6 per group) detected 3499 metabolic features, of which 1292 were retained after QC-based reproducibility and blank filtering. A total of 109 metabolites were annotated, and 53 met the criteria of an adjusted p-value < 0.05 with a fold change above 1.5 (increased) or below 0.67 (approximately 1/1.5; decreased) in the comparison between LPS and LPS + caffeine groups. After excluding 19 exogenous, medium-derived, or less interpretable annotations, 34 metabolites (17 increased, 17 decreased) were retained for interpretation. The caffeine-associated profile was mainly characterized by alterations in nucleotide-sugar, purine-related, glutamine/glutamate-associated amino acid, redox-related, and central carbon metabolism, together with lipid remodeling. Pathway-level analysis further supported the involvement of glyoxylate and dicarboxylate metabolism, glycerophospholipid metabolism, amino sugar and nucleotide sugar metabolism, and alanine/aspartate/glutamate metabolism. Because LPS signaling is initiated at the TLR4/MD-2 complex, we used molecular docking to explore a possible upstream basis for these changes. Docking suggested that caffeine may interact with residues located near the TLR4/MD-2 ligand-recognition region. Overall, these findings indicate that caffeine treatment is associated with coordinated intracellular metabolic remodeling in LPS-stimulated RAW 264.7 macrophages.

Keywords: *Caffeine, RAW 264.7 macrophages, untargeted metabolomics, LC–QTOF–MS, TLR4/MD-2, molecular docking.*

RAW 264.7 Makrofaj Hücrelerinde Kafein İlişkili Metabolik Değişikliklerin LC–MS Temelli Hedeflenmemiş Metabolomik ile Karakterizasyonu

ÖZ

Kafein, yaygın olarak tüketilen ve immünomodülatör özelliklere sahip olduğu bildirilen bir metilksantindir. Bununla birlikte, inflamasyonla ilişkili metabolik yeniden programlanma üzerindeki kapsamlı etkileri henüz tam olarak aydınlatılamamıştır. Bu çalışmada, lipopolisakkarit (LPS) ile uyarılmış RAW 264.7 makrofajlarında kafeine bağlı metabolik değişiklikler, LC–MS tabanlı hedefsiz hücre içi metabolomik analizler kullanılarak araştırılmıştır. Hücre canlılığı analizleri, 0,2 mM kafeinin kontrol hücreleriyle karşılaştırılabilir düzeyde canlılığı koruduğunu göstermiş ve metabolomik analizler için bu konsantrasyon seçilmiştir. Hedeflenmemiş LC–QTOF–MS profillemesi (grup başına n = 6) sonucunda 3499 pik tespit edilmiş, bunlardan 1292'si kalite kontrol (QC) temelli tekrarlanabilirlik ve kör (blank) örnek filtreleme kriterlerini karşılayarak analize dahil edilmiştir. Toplam 109 metabolit tanımlanmış olup, bunlardan 53'ü LPS ile LPS + kafein grupları arasındaki karşılaştırmada düzeltilmiş p değeri < 0,05 ve değişim katsayısı (fold change) >1,5 (artış) veya <0,67 (azalış; 1/1,5) kriterlerini karşılamıştır. Eksojen kaynaklı, besiyerinden türeyen veya biyolojik olarak yorumlanması sınırlı olan 19 anotasyonun çıkarılmasının ardından, yorumlamaya 34 metabolit (17'si artmış, 17'si azalmış) dahil edilmiştir. Kafeinle ilişkili metabolik profil; başlıca nükleotid-şeker metabolizması, pürin metabolizması, glutamin/glutamat ile ilişkili amino asit metabolizması, redoks metabolizması ve merkezi karbon metabolizmasının yanı sıra lipit yeniden yapılanmasındaki değişikliklerle karakterize edilmiştir. Yolak düzeyindeki analizler ayrıca glikoksilat ve dikarboksilat metabolizması, gliserofosfolipit metabolizması, amino şeker ve nükleotid şeker metabolizması ile alanin/aspartat/glutamat metabolizmasının bu süreçte rol oynadığını desteklemiştir. LPS aracılı sinyal iletimi TLR4/MD-2 kompleksi üzerinden başlatıldığından, gözlenen metabolik değişikliklerin olası üst akış mekanizmasını araştırmak amacıyla moleküler kenetlenme analizleri gerçekleştirilmiştir. Kenetlenme analizi, kafeinin TLR4/MD-2 kompleksinin ligand tanıma bölgesine yakın konumlanan amino asit kalıntıları ile etkileşime girebileceğini göstermiştir. Genel olarak bu bulgular, kafein uygulamasının LPS ile uyarılmış RAW 264.7 makrofajlarında koordineli bir hücre içi metabolik yeniden yapılanma ile ilişkili olduğunu ortaya koymaktadır.

Anahtar Kelimeler: *Kafein, RAW 264.7 makrofaj hücreleri, hedeflenmemiş metabolomik, LC–QTOF–MS, TLR4/MD-2, moleküler kenetleme*

Recieved: 03.08.2026
Revised: 01.09.2026
Accepted: 08.09.2026

[*] ORCID: 0000-0001-7429-9349, Hacettepe University, Faculty of Pharmacy, Department of Analytical Chemistry, 06100 Ankara, Türkiye
[**] ORCID: 0000-0001-6311-5399, Hacettepe University, Faculty of Pharmacy, Department of Pharmaceutical Chemistry, 06100 Ankara, Türkiye
[***] ORCID: 0000-0003-4135-3497, Hacettepe University, Faculty of Pharmacy, Department of Pharmacognosy, 06100 Ankara, Türkiye

[°] Corresponding Author; Ozan Kaplan
E-mail: ozankaplan@hacettepe.edu.tr

INTRODUCTION

Metabolomics systematically characterizes low-molecular-weight metabolites in cells, tissues, biofluids, or organisms. Because metabolites are downstream products of genomic, transcriptomic, proteomic, and environmental regulation, metabolomic profiling provides a close functional readout of the biochemical state of a biological system and is highly sensitive to physiological or pathological perturbation (Fiehn, 2002; Nicholson, Lindon, & Holmes, 1999; Patti, Yanes, & Siuzdak, 2012). As a discovery-driven strategy, LC–MS-based untargeted metabolomics allows broad detection of endogenous metabolites and comprehensive assessment of metabolic signatures associated with disease models, pharmacological interventions, and cellular phenotypes (Čuperlović-Culf, Barnett, Culf, & Chute, 2010; Dunn, Bailey, & Johnson, 2005). In cell culture, this approach offers reduced biological variability, standardized treatment conditions, and controlled exposure times, and is particularly suited to characterizing changes in central carbon metabolism, amino acid metabolism, nucleotide turnover, redox balance, lipid remodeling, and energy-related pathways (Domenick, Gill, Vedam-Mai, & Yost, 2021; Zhang, Sun, Xu, Qiu, & Wang, 2013).

Inflammation is a regulated response initiated by pathogenic, autoimmune, or physical stimuli, involving coordinated biochemical events that vary with the triggering factor (Gusev & Zhuravleva, 2022). Macrophages are central mediators, contributing to chemokine and cytokine production, phagocytic activity, control of tissue damage, and the transition from inflammation to tissue repair, and can acquire distinct functional phenotypes depending on the local microenvironment and activating stimulus (Arroyo-Xochihua, Zepeda, & Sánchez-Medina, 2026; Meizlish, Franklin, Zhou, & Medzhitov, 2021). RAW 264.7 murine macrophages are widely used to study these responses, offering continuous proliferation, reduced donor-to-donor variability, and reported phenotypic and functional stability across serial passages (Taciak et al., 2018); following LPS stimulation, they undergo characteristic metabolic adaptations involving amino acid, purine, and energy metabolism.

In macrophages, inflammatory activation is closely coupled to metabolic reprogramming. Upon exposure to pro-inflammatory stimuli, macrophages shift their metabolic state to support rapid effector functions, including cytokine production, nitric oxide (NO) synthesis, reactive oxygen species (ROS) generation, and lipid mediator formation, through coordinated changes in glycolysis, the tricarboxylic acid cycle, the pentose phosphate pathway, amino acid metabolism, and lipid metabolism (Jha et al., 2015; Kelly & O'Neill, 2015; O'Neill, Kishton, & Rathmell, 2016). In LPS-activated macrophages, increased glycolytic activity and altered mitochondrial metabolism are commonly observed, and specific TCA cycle intermediates such as citrate, succinate, and itaconate may act not only as metabolic intermediates but also as regulators of inflammatory signaling (Lampropoulou et al., 2016; Mills et al., 2018; Tannahill et al., 2013).

Among the stimuli that induce this reprogramming, LPS is the most extensively studied activator of macrophages. LPS initiates inflammatory signaling by binding the Toll-like receptor 4/myeloid differentiation factor 2 (TLR4/MD-2) receptor complex, triggering MyD88- and TRIF-dependent cascades that lead to NF-κB and MAPK activation and the production of pro-inflammatory mediators including inducible NO synthase (iNOS), cyclooxygenase-2 (COX-2), tumor necrosis factor-α, interleukin (IL)-1β, and IL-6 (Akira & Takeda, 2004; Lu, Yeh, & Ohashi, 2008; Molteni, Gemma, & Rossetti, 2016; Park et al., 2009). Because TLR4/MD-2 activation is an early event in this cascade, the complex provides a relevant structural target for exploratory molecular interaction analysis, and integrating intracellular metabolomic profiling with molecular docking may therefore provide complementary information on downstream metabolic alterations and possible upstream ligand–receptor interactions.

Caffeine (1,3,7-trimethylxanthine) is a naturally occurring methylxanthine alkaloid found in coffee, tea, and several other dietary sources (Daly, 2007; Fredholm, Bättig, Holmén, Nehlig, & Zvartau, 1999). Beyond its stimulant properties, it influences multiple cellular processes mainly through non-selective antagonism of adenosine receptors, with phosphodiesterase inhibition, intracellular cyclic AMP modulation, and calcium-related signaling becoming relevant depending on the experimental concentration (Jacobson, Gao, Matricon, Eddy, & Carlsson, 2022). Since adenosine signaling is closely involved in the regulation of immune and inflammatory responses, caffeine has attracted attention as a bioactive compound with potential immunomodulatory properties (Haskó, Linden, Cronstein, & Pacher, 2008). In LPS-stimulated RAW 264.7 macrophages, caffeine has been reported to reduce NO production, downregulate mediators such as iNOS, COX-2, and selected interleukins, and modulate NF-κB- and MAPK-related signaling (Hwang, Kim, Ryu, & Lee, 2016). However, these effects may be context-dependent, as different macrophage subpopulations can exhibit distinct cytokine and inflammasome-related responses to caffeine (Kovács et al., 2021).

Although previous studies have reported that caffeine can modulate inflammatory mediator production in LPS-stimulated macrophages, its broader influence on inflammation-associated metabolic reprogramming remains poorly understood. Given its widespread dietary consumption and reported immunomodulatory properties, characterization of caffeine-associated metabolic alterations may provide additional insight into its effects under inflammatory conditions. LC–MS-based untargeted metabolomics provides a comprehensive strategy for characterizing these global biochemical changes; however, metabolomic analysis alone cannot establish the upstream molecular mechanisms responsible for the observed alterations. Since activation of the TLR4/MD-2 receptor complex represents an early event in LPS-induced inflammatory signaling, molecular docking was employed as an exploratory computational approach to evaluate a possible interaction of caffeine with this receptor complex. Therefore, the present study combined LC–MS-based untargeted metabolomics to characterize caffeine-associated metabolic alterations in LPS-stimulated RAW 264.7 macrophages with exploratory molecular docking to investigate a possible interaction with the TLR4/MD-2 ligand-recognition region.

MATERIALS AND METHODS

Chemicals and reagents

Methanol, acetonitrile, MTT [3-(4,5-dimethylthiazol-2-yl)-2,5-diphenyl tetrazolium bromide], fetal bovine serum (FBS), Dulbecco's Modified Eagle Medium (DMEM), and LPS were purchased from Sigma (St. Louis, MO, USA). Anhydrous caffeine (98.5% purity) was obtained from Carlo Erba (Val-de-Reuil, France), phosphoric acid and LC–MS grade formic acid from Merck (Darmstadt, Germany), trypsin–EDTA (0.25%) from Biowest SAS (Nuaillé, France), penicillin–streptomycin solution (100×) from Capricorn Scientific GmbH (Ebsdorfergrund, Germany), and dimethyl sulfoxide (DMSO) from Isolab (Germany).

Cell culture and viability assay

RAW 264.7 macrophages were maintained in DMEM supplemented with 10% FBS and 1% antibiotic solution under standard culture conditions (37 °C, 5% CO_2, humidified atmosphere). Cells were subcultured every 2 days and used for experiments during the exponential growth phase.

For viability assessment, cells were seeded into 96-well plates at 8×10^5 cells/mL and allowed to attach for 24 h. The medium was replaced with fresh medium containing caffeine (0.05–1 mM) for 24 h. The cells were then washed and incubated with MTT solution (10 µL, 5 mg/mL) for 4–6 h. Formazan crystals were dissolved in 100 µL DMSO, and absorbance was recorded at 570/620 nm using a microplate reader (Doğan, Kutluay, Genç, & Saraçoğlu, 2023). Viability was expressed relative to untreated control cells. Ex-

periments were performed independently three times with triplicate measurements, and data are presented as mean ± SD.

Intracellular metabolite extraction

RAW 264.7 cells were plated in 24-well plates at 8×10^5 cells/mL and maintained for 24 h at 37 °C in a humidified incubator with 5% CO_2. Two experimental groups were prepared: LPS alone and LPS + caffeine, each consisting of six independent biological replicates. Following the initial incubation period, the culture medium was replaced with fresh treatment medium. In the LPS group, cells were treated with LPS at a final concentration of 0.1 μg/mL, whereas cells in the LPS + caffeine group were co-treated with LPS (0.1 μg/mL) and caffeine (0.2 mM) for 24 h. The caffeine concentration was selected based on the MTT viability assay, in which 0.2 mM caffeine without LPS preserved cell viability at a level comparable to untreated control cells. The medium was then removed, and the cells were gently washed with phosphate-buffered saline (PBS) to eliminate residual medium components. Cellular metabolism was quenched by briefly cooling the plates with liquid nitrogen, and intracellular metabolites were extracted by adding 750 μL of ice-cold methanol directly to each well, followed by cell scraping. The wells were rinsed with an additional 500 μL of ice-cold methanol to improve recovery. The combined extracts were centrifuged at 9000 rpm for 10 min to remove cellular debris, and 1000 μL of the supernatant was evaporated to dryness in a vacuum concentrator at 4 °C. The residues were reconstituted in 200 μL of acetonitrile–water (70:30, v/v) and vortex-mixed before LC–MS analysis. A pooled QC sample was prepared from equal aliquots of all extracted samples.

LC-MS analysis

Metabolomic profiling was performed using an Agilent 1290 Infinity II LC system coupled to an Agilent 6530 Q-TOF mass spectrometer equipped with a dual electrospray ionization source. Chromatographic separation was achieved on a Waters XBridge BEH C18 column (2.1 × 100 mm, 2.5 μm) maintained at 35 °C, while the autosampler temperature was kept at 4 °C. The mobile phases were water containing 0.1% formic acid (solvent A) and acetonitrile containing 0.1% formic acid (solvent B). The flow rate was set to 0.3 mL/min, and the injection volume was 2 μL.

The chromatographic gradient was as follows: 0–2 min, 95% A; 2–10 min, linear decrease from 95% A to 5% A; 10–12 min, 5% A; 12.1 min, return to 95% A; and 12.1–20 min, re-equilibration at 95% A. Mass spectrometric detection was performed in negative electrospray ionization mode using full-scan acquisition over an m/z range of 75–1200. Negative ESI mode was selected because the applied chromatographic and mass spectrometric conditions provided suitable coverage of several metabolite classes relevant to the present study, including organic acids, nucleotide-related metabolites, selected amino acid-related metabolites, fatty acids, phospholipids, and sphingolipid-related metabolites. Mass spectrometric source parameters were as follows: capillary voltage, 3500 V; fragmentor voltage, 175 V; skimmer voltage, 65 V; octopole RF peak, 750 V; drying gas temperature, 300 °C; drying gas flow, 8 L/min; and nebulizer pressure, 35 psig. Full-scan MS1 data were acquired at a scan rate of 1.0 spectrum/s. Reference mass correction was not enabled during acquisition. The Q-TOF mass spectrometer was calibrated before analysis to ensure mass accuracy, and the same acquisition parameters were applied throughout the analytical sequence.

Mobile phase blank and pooled QC injections were included after every six sample injections to monitor background signals, carryover, and analytical stability, and the sample injection order was randomized to minimize run-order-related bias.

LC-MS data processing

Raw LC–MS data were processed in MZmine

2.53 through mass detection, chromatogram building, deconvolution, isotope grouping, retention time alignment, gap filling, and peak area extraction. Mass detection used an intensity threshold of 1.0×10^3; chromatogram building used an m/z tolerance of 10 ppm; deconvolution used the local minimum search algorithm; isotope grouping used an m/z tolerance of 10 ppm with a retention time tolerance of 0.1 min; and feature alignment used the join aligner algorithm with an m/z tolerance of 0.01 Da and a retention time tolerance of 0.2 min, followed by gap filling to recover missing peak areas.

Pooled QC injections were used to evaluate analytical reproducibility, and features with a relative standard deviation greater than 30% in pooled QC injections were excluded. Mobile phase blank injections were used to identify background signals and contaminants; after QC-based filtering, features were retained only when their abundance in biological samples was at least three-fold higher than in blank injections. The filtered peak area table was then exported for statistical analysis.

Statistical analysis

The filtered peak area matrix was imported into MetaboAnalyst for statistical analysis and visualization. Each biological replicate was injected twice, and these technical replicate injections were averaged, yielding six values per experimental group; the matrix was then normalized to the total peak area of each sample. Principal component analysis (PCA) was first performed as an unsupervised multivariate method to evaluate sample distribution, group-related metabolic variation, analytical reproducibility of QC injections, and potential outliers.

Univariate statistical analysis compared the LPS and LPS + caffeine groups using a two-sample t-test. Fold changes were calculated as the ratio of abundance in the LPS + caffeine group to that in the LPS group, with values greater than 1 indicating increased abundance and values less than 1 indicating decreased abundance after caffeine treatment.

For multiple testing correction, p-values were adjusted using the Benjamini–Hochberg procedure, and metabolic features were considered differentially altered when fold change was > 1.5 or < 0.67 with an adjusted p-value < 0.05. Volcano plots were generated to display $\log_2$ fold change against statistical significance, and a lollipop plot was generated from the $\log_2$ fold change values of the curated annotated metabolites to show the direction and magnitude of caffeine-associated alterations.

Partial least squares-discriminant analysis (PLS-DA) was used as a complementary supervised multivariate method, with model performance assessed by cross-validated accuracy, R^2, and Q^2 values, and class discrimination tested against random group assignment using 1000 permutations. Variable importance in projection (VIP) scores were examined as supplementary information and were not used as the sole criterion for metabolite selection; final biological interpretation was based primarily on statistically significant, annotated, and biologically curated metabolites.

Metabolite annotation and pathway analysis

Metabolite annotation used an in-house LC–MS metabolite library and complementary public databases. Detected features were first matched against the in-house library on accurate m/z values and retention times obtained under the same chromatographic and mass spectrometric conditions; those matching authentic reference standards in both accurate mass and retention time were reported as MSI level 1 annotations.

Features not confirmed by authentic reference standards were assigned as putative annotations based on accurate mass matching, isotope and adduct information, chromatographic behavior, and database support from HMDB, KEGG, METLIN, and LIPID MAPS. Because data-dependent MS/MS acquisition was not performed, we interpreted putative annotations cautiously and did not consider them structural-

ly confirmed; interpretation therefore prioritized metabolites with higher annotation confidence, endogenous relevance to RAW 264.7 macrophage metabolism, and consistency with pathway-level patterns. Supplementary Table S2 provides additional annotation information for curated metabolites retained for biological interpretation, including observed m/z, retention time, mass error, MSI annotation level, annotation evidence, and curation/caution notes.

To reduce the risk of overinterpretation, annotations considered likely exogenous, medium- or FBS-derived, treatment-related, stereochemically ambiguous, or biologically less interpretable in intracellular RAW 264.7 macrophage metabolism were excluded, leaving a curated list of 34 significantly altered annotated metabolites.

The curated metabolites were analyzed using MetaboAnalyst, with pathway mapping based on KEGG and HMDB identifiers where available. Pathway-level p-values were adjusted for multiple testing using the false discovery rate (FDR) method. Both raw and FDR-adjusted p-values are reported in Table 1. Pathway-level results were interpreted considering raw and FDR-adjusted p-values, pathway impact, the number of matched metabolites, annotation confidence, and biological relevance to macrophage activation and the metabolic domains examined here.

Molecular docking studies

Molecular docking was performed as an exploratory computational approach to evaluate a possible interaction of caffeine with the ligand-recognition region of the TLR4/MD-2 complex. The crystal structure of the TLR4/MD-2 complex was retrieved from the Protein Data Bank (PDB ID: 3FXI) (Park et al., 2009); it contains a co-crystallized native ligand within the ligand-recognition region and was therefore selected as the receptor model. Protein preparation was performed with the Protein Preparation Wizard in Schrödinger Maestro (Schrödinger, LLC, 2023), assigning bond orders, adding missing hydrogen atoms, and generating protonation states of ionizable residues under physiological conditions. Crystallographic water molecules farther than 5 Å from the co-crystallized ligand were removed, and the prepared structure was subjected to restrained energy minimization using the OPLS5 force field.

The two-dimensional structure of caffeine was constructed and prepared using the LigPrep module of Schrödinger Maestro (Schrödinger, LLC, 2019). During ligand preparation, the corresponding three-dimensional structure was generated and subsequently energy-minimized using the OPLS5 force field.

Docking calculations were carried out with the Glide module in Schrödinger Maestro (Friesner et al., 2004). The receptor grid was centered on the coordinates of the co-crystallized native ligand, thereby defining the experimentally resolved ligand-binding region of the TLR4/MD-2 complex. The protocol was validated by re-docking the co-crystallized ligand into the TLR4–MD-2 binding site and confirming reproduction of its experimentally observed binding pose. Binding poses generated for caffeine were ranked by their Glide docking scores, and the top-ranked predicted pose was selected for interaction analysis.

RESULTS

Effect of caffeine on cell viability

The effect of caffeine alone, in the absence of LPS stimulation, on the viability of RAW 264.7 macrophages was evaluated using the MTT assay. Caffeine at 0.05 mM slightly increased viability (approximately 110%), whereas 0.2 mM maintained viability comparable to the control group (approximately 98%) (Figure 1.). Higher concentrations reduced viability in a concentration-dependent manner: viability was approximately 84% and 67% at 0.5 and 1 mM, respectively. These findings indicate that higher caffeine concentrations may reduce RAW 264.7 cell viability.

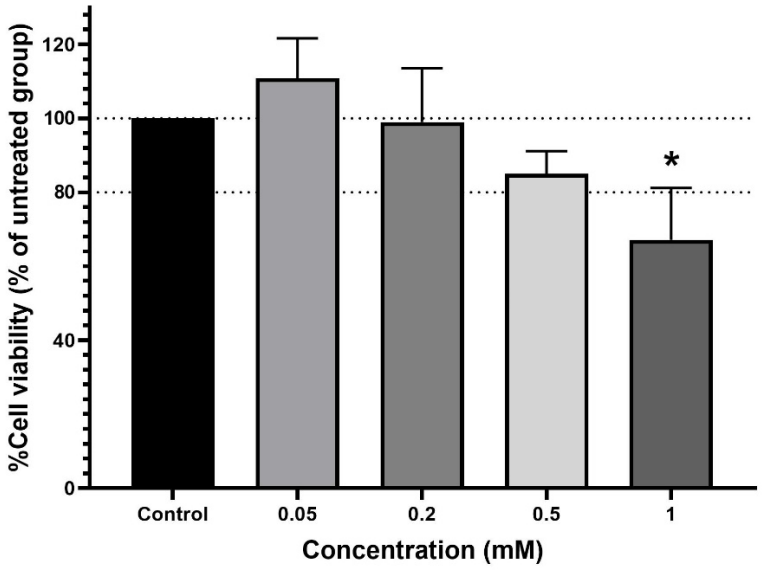

Figure 1. Effect of caffeine on the viability of RAW 264.7 macrophages. Cells were treated with caffeine at concentrations of 0.05, 0.2, 0.5, and 1 mM for 24 h, and cell viability was determined using the MTT assay. Cell viability was expressed as a percentage relative to the untreated control group, which was set at 100%. Data are presented as mean ± SD of three independent experiments performed in triplicate. Statistical analysis was performed using one-way ANOVA followed by a post hoc Dunnett's test ($p < 0.05$ compared with the untreated control group)

LC-MS-based intracellular metabolomic profiling

LC–MS-based untargeted intracellular metabolomic analysis was performed to investigate metabolic alterations associated with caffeine treatment in LPS-stimulated RAW 264.7 macrophages. The study included two experimental groups: LPS-stimulated cells and LPS-stimulated cells treated with caffeine.

In the initial untargeted data matrix, 3499 metabolic features were detected. After QC-based reproducibility filtering and blank filtering, 1292 metabolic features were retained for subsequent statistical analysis. These filtering steps reduced non-reproducible and background-derived signals and provided a reliable feature matrix for downstream multivariate and univariate statistical analyses.

Multivariate analysis of intracellular metabolomic profiles

Principal component analysis (PCA) was performed to evaluate the global distribution of intracellular metabolomic profiles from the LPS and LPS + caffeine groups, together with pooled QC samples. The pooled QC samples formed a tight cluster relative to the biological samples, supporting acceptable analytical reproducibility throughout the LC–MS sequence. The PCA model showed that the LPS + caffeine group displayed a distinct metabolic distribution relative to the LPS group, while the pooled QC samples formed a relatively tight cluster. PC1 and PC2 explained 16.8% and 11.5% of the total variance, respectively (Figure 2.), indicating caffeine-associated metabolic differences under LPS-stimulated conditions. PLS-DA provided a complementary supervised assessment of group discrimination. Cross-validation showed high model performance, with accuracy and R^2 close to 1.0 and Q^2 of approximately 0.98 (Supplementary Figure S1.). Permutation testing using 1000 permutations gave $R^2Y = 0.998$ and $Q^2 = 0.981$ for the original model, with permutation p-values of 0.003 for both parameters (Supplementary Figure S2.), indicating that the observed group discrimination was unlikely to be explained by random class assignment. We interpreted the PLS-DA results as supplementary evidence.

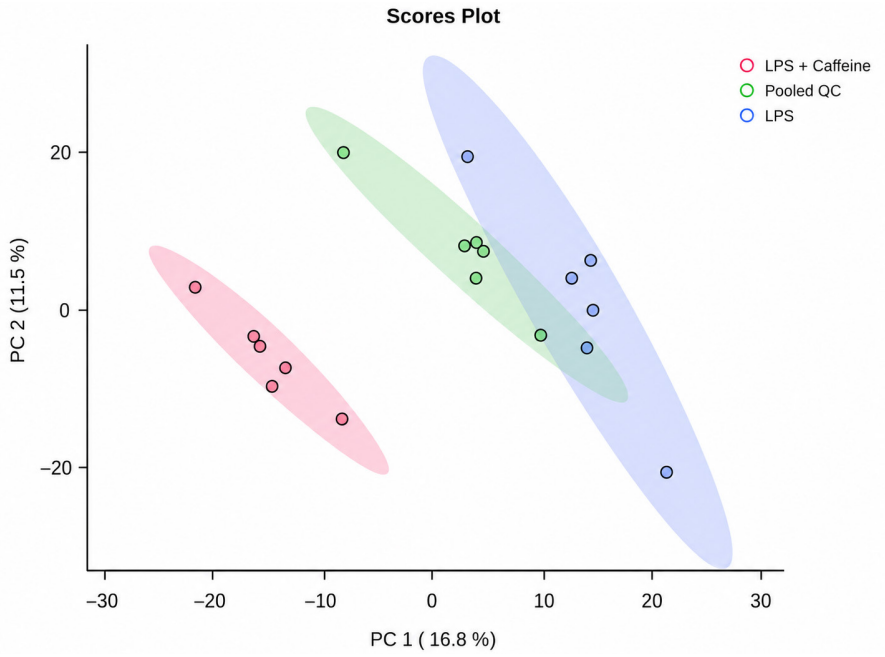

Figure 2. PCA score plot of intracellular metabolomic profiles from the LPS group, the LPS + caffeine group, and pooled QC samples. PC1 and PC2 explained 16.8% and 11.5% of the total variance, respectively. The pooled QC samples formed a relatively tight cluster, supporting analytical reproducibility throughout the LC–MS sequence. Ellipses are shown as visual guides to illustrate the distribution of samples within each group

Volcano plot analysis revealed a broad distribution of altered metabolic features between the LPS and LPS + caffeine groups (Figure 3.). Among the 1292 retained features, several showed marked changes in abundance following caffeine treatment, and these altered features were subsequently annotated.

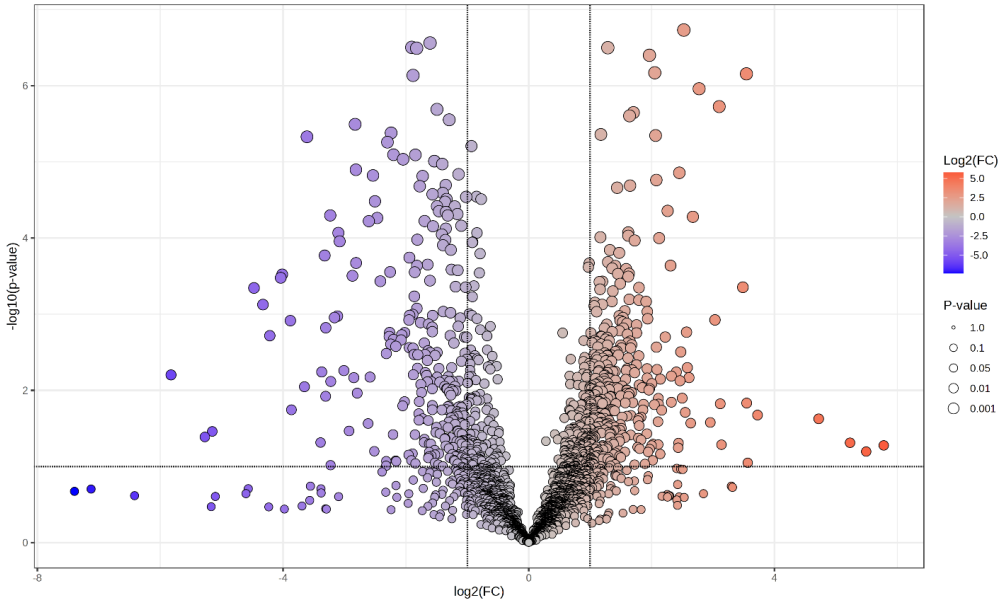

Figure 3. Volcano plot showing differentially altered metabolic features between the LPS and LPS + caffeine groups. The x-axis represents $\log_2$ fold change, and the y-axis represents $-\log_{10}$(p-value). Metabolite annotation focused on features meeting the selected fold-change and significance thresholds

A total of 109 metabolites were annotated using the in-house LC–MS library and complementary metabolite databases, of which 53 met the statistical criteria in the comparison between the LPS and LPS + caffeine groups. After curation, 34 metabolites were retained for biological interpretation: 17 increased and 17 decreased in the LPS + caffeine group relative to the LPS group (Supplementary Table S1.). Supplementary Table S2 provides additional annotation information for these curated metabolites, including observed m/z, retention time, mass error, MSI annotation level, annotation evidence, and curation/caution notes. Metabolites with potential isomeric ambiguity are indicated in Supplementary Table S2 and were interpreted cautiously in the Discussion.

A lollipop plot of the 34 curated metabolites illustrated the direction and magnitude of the caffeine-associated metabolic changes (Figure 4.). The balanced pattern of increased and decreased metabolites supports the interpretation that caffeine treatment was associated with broad intracellular metabolic remodeling rather than a change limited to a single metabolic class.

Pathway-level analysis of the curated metabolites identified glyoxylate and dicarboxylate metabolism, glycerophospholipid metabolism, nitrogen metabolism, amino sugar and nucleotide sugar metabolism, alanine/aspartate/glutamate metabolism, arginine biosynthesis, and glycerolipid metabolism with raw p-values < 0.05. However, none of the evaluated pathways remained statistically significant after FDR correction (FDR-adjusted $p > 0.05$ for all pathways; Table 1.). Accordingly, we interpreted these pathway-level findings as exploratory patterns of metabolite representation rather than statistically confirmed pathway enrichment. The observed patterns were nevertheless consistent with the metabolite-level alterations involving central carbon, amino acid, redox-associated, nucleotide-sugar, and lipid-related metabolic domains in LPS-stimulated RAW 264.7 macrophages.

Table 1. Selected biologically relevant pathways represented among curated metabolites altered between LPS and LPS + caffeine groups

Pathway name	Hits / Total	Raw p-value	FDR-adjusted p-value	Impact	Biological relevance
Glyoxylate and dicarboxylate metabolism	4/32	0.002893	0.13987	0.080	Central carbon/organic acid metabolism
Glycerophospholipid metabolism	4/36	0.004487	0.13987	0.282	Membrane lipid remodeling
Nitrogen metabolism	2/6	0.005245	0.13987	0.000	Amino acid and nitrogen balance
Amino sugar and nucleotide sugar metabolism	4/42	0.007856	0.15712	0.105	Nucleotide-sugar and glycosylation-related metabolism
Alanine, aspartate and glutamate metabolism	3/28	0.015758	0.25213	0.311	Glutamine/glutamate-associated metabolism
Arginine biosynthesis	2/14	0.028876	0.38502	0.122	Nitrogen and inflammatory mediator-related metabolism
Glycerolipid metabolism	2/16	0.037171	0.38578	0.056	Lipid remodeling
Citrate cycle (TCA cycle)	2/20	0.056091	0.44873	0.135	Mitochondrial central carbon metabolism
Glutathione metabolism	2/28	0.101430	0.67621	0.276	Redox-associated metabolism
Sphingolipid metabolism	2/32	0.126940	0.78116	0.038	Sphingolipid-associated signaling

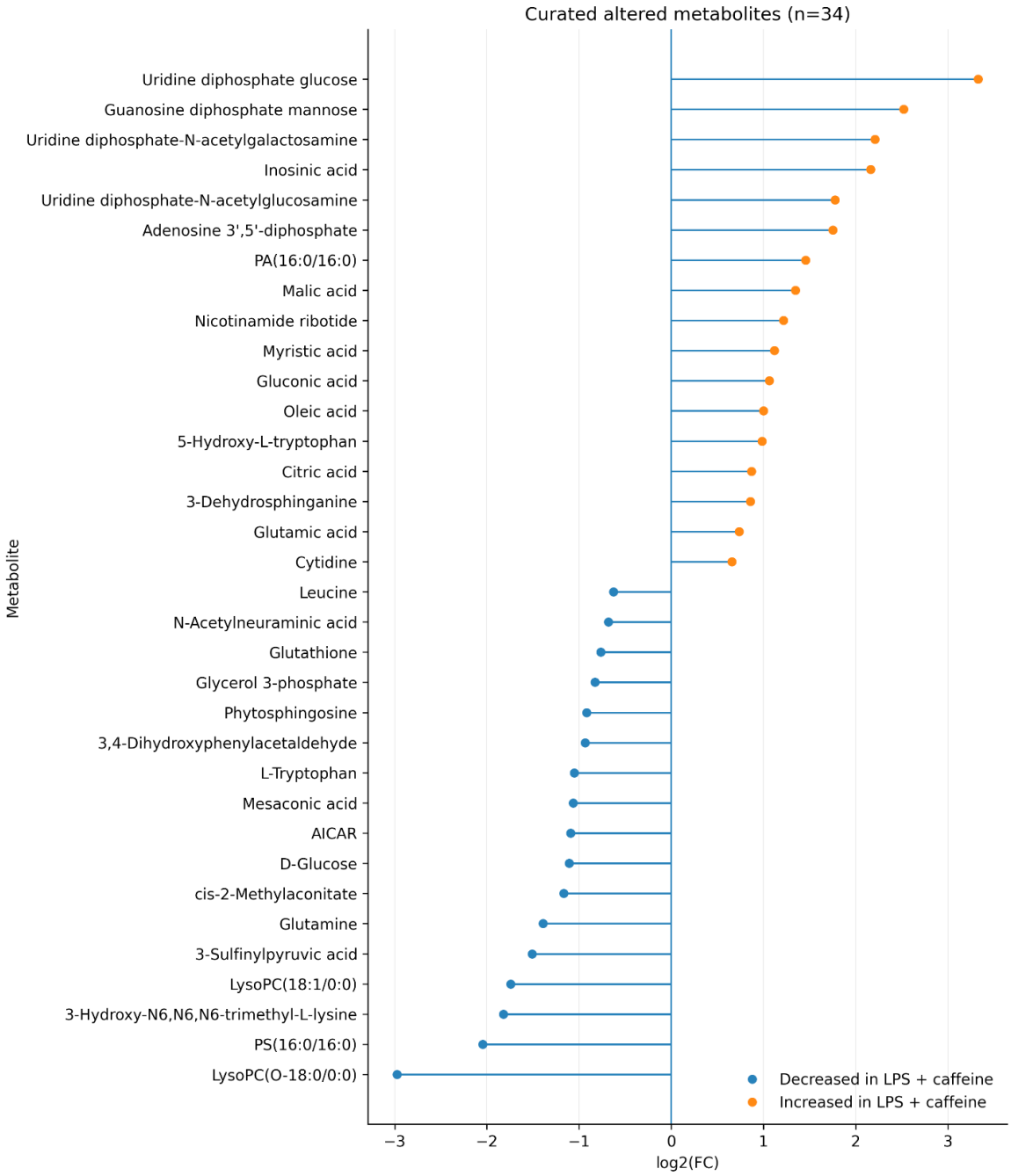

Figure 4. Lollipop plot showing $\log_2$(fold change) values of 34 curated metabolites altered between LPS and LPS + caffeine groups. Positive $\log_2$(FC) values indicate metabolites increased in the LPS + caffeine group, whereas negative values indicate metabolites decreased after caffeine treatment. Metabolites shown in the figure were retained after exclusion of annotations considered exogenous, stereochemically ambiguous, putative/suspicious, or biologically less interpretable for intracellular RAW 264.7 macrophage metabolism

Molecular docking studies

Molecular docking was used to explore whether caffeine could occupy the ligand-recognition region of the TLR4/MD-2 complex; the predicted binding mode and surrounding amino acid residues are described below.

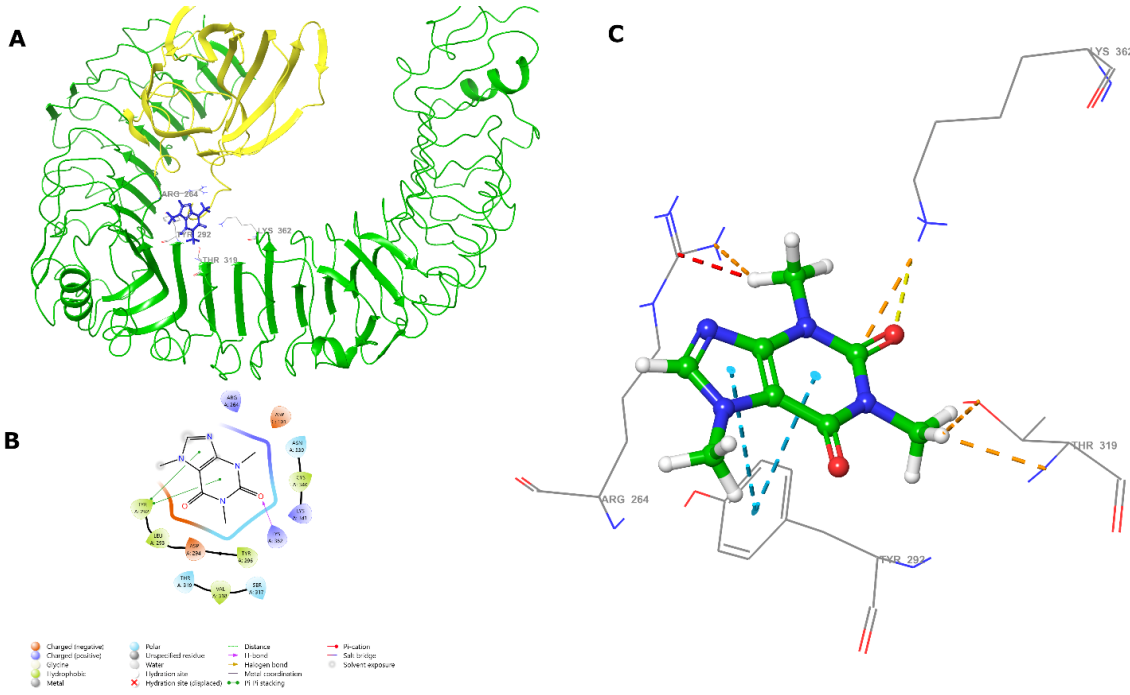

Figure 5. Molecular docking analysis of caffeine within the TLR4/MD-2 complex (PDB ID: 3FXI). (A) Overall binding pose of caffeine located at the TLR4/MD-2 ligand-recognition interface. TLR4 and MD-2 are shown as cartoon representations, while caffeine is displayed as blue sticks. (B) Two-dimensional interaction diagram illustrating the interactions between caffeine and the surrounding amino acid residues within the binding pocket. (C) Three-dimensional close-up view of the predicted binding mode

Following docking calculations, the top-ranked predicted caffeine pose yielded a Glide docking score of −6.05. The predicted binding pose positioned caffeine near the TLR4–MD-2 interface and suggested possible hydrogen-bonding, aromatic, and hydrophobic contacts with surrounding residues (Figure 5). When the interactions of caffeine with the TLR4/MD-2 complex were examined, the carbonyl oxygen atom of caffeine formed a conventional hydrogen bond with Lys362, providing an important anchoring interaction within the binding pocket. In addition, the fused xanthine ring established a π–π stacking interaction with Tyr292, while Thr319 remained near the ligand and contributed a weak polar interaction. Although no direct interaction with Arg262 was observed, preservation of the remaining three critical residues is consistent with structural compatibility of caffeine with the ligand-recognition region of the TLR4/MD-2 complex.

In addition to these conserved interactions, caffeine was surrounded by Arg264, Leu293, Asp294, Tyr296, Val318, Asn339, Cys340, and Lys341 of TLR4, along with Asp101 of MD-2, which collectively define the physicochemical environment of the binding pocket (Figure 5.). Although these residues did not form classical hydrogen bonds, they remained near the docked ligand and may participate in hydrophobic, electrostatic, or van der Waals interactions. The proximity of residues from both TLR4 and MD-2 suggests that the predicted caffeine pose lies near the receptor-recognition interface rather than being associated exclusively with either protein component.

Interestingly, unlike the crystallographic antagonist Eritoran or the lipid A moiety of LPS, which deeply occupy the extended hydrophobic cavity of MD-2, caffeine adopted a more surface-oriented binding mode near the TLR4–MD-2 interface.

DISCUSSION

In the present study, LC–MS-based untargeted intracellular metabolomics was used to investigate caffeine-associated metabolic modulation in LPS-stimulated RAW 264.7 macrophages. In the viability assay, which evaluated caffeine without LPS stimulation, 0.2 mM caffeine preserved RAW 264.7 cell viability at a level comparable to untreated control cells. This non-cytotoxic concentration was therefore selected for the subsequent metabolomic experiment, in which LPS-stimulated cells were compared in the absence or presence of caffeine. The untargeted LC–MS workflow detected 3499 metabolic features, of which 1292 were retained after QC-based reproducibility filtering and blank filtering, providing a reliable feature matrix for downstream statistical analysis.

Multivariate analysis showed that caffeine treatment was associated with a distinct intracellular metabolic distribution under LPS-stimulated conditions. The supervised PLS-DA model further supported group discrimination, and permutation testing indicated that the observed separation was unlikely to result from random class assignment. However, we interpreted the PLS-DA findings as supplementary evidence and based biological interpretation primarily on statistically significant, annotated, and biologically curated metabolites.

Among 109 annotated metabolites, 53 met the statistical criteria in the LPS versus LPS + caffeine comparison. After biological curation and exclusion of annotations considered exogenous, medium/FBS-derived, treatment-related/xenobiotic, stereochemically ambiguous, putative/suspicious, or less interpretable in the context of intracellular RAW 264.7 macrophage metabolism, 34 metabolites were retained for interpretation. These curated metabolites showed a balanced pattern of increased and decreased abundance, indicating that caffeine treatment was associated with coordinated metabolic remodeling rather than a unidirectional metabolic response.

Macrophage activation is closely linked to metabolic reprogramming. Pro-inflammatory stimulation by LPS is known to induce coordinated changes in central carbon metabolism, amino acid metabolism, nucleotide metabolism, redox homeostasis, and lipid mediator-related pathways (Jha et al., 2015; Kelly & O'Neill, 2015; Lampropoulou et al., 2016; Mills et al., 2018; O'Neill et al., 2016; Tannahill et al., 2013). These metabolic adaptations support inflammatory mediator production, oxidative stress responses, membrane remodeling, and immune effector functions (Jha et al., 2015; Kelly & O'Neill, 2015; O'Neill et al., 2016). In this context, the altered nucleotide-sugar metabolites, glutamine/glutamate-related metabolites, organic acids, glutathione, lysophospholipids, phosphatidic acid, and sphingolipid-related metabolites observed in the present study suggest that caffeine treatment reshaped multiple interconnected metabolic domains involved in LPS-associated macrophage activation.

Caffeine is a methylxanthine compound structurally related to purine metabolism and is widely recognized as a non-selective adenosine receptor antagonist (Daly, 2007; Fredholm et al., 1999; Jacobson et al., 2022). Adenosine receptor signaling plays an important role in the regulation of immune and inflammatory responses (Haskó et al., 2008; Jacobson et al., 2022). In LPS-stimulated RAW 264.7 macrophages, caffeine has previously been reported to modulate NO production and inflammatory mediators such as iNOS, COX-2, and IL-6, partly through NF-κB- and MAPK-related signaling pathways (Hwang et al., 2016). However, caffeine-mediated immune effects may be context-dependent, as different macrophage populations can exhibit distinct cytokine and inflammasome-related responses to caffeine exposure (Kovács et al., 2021). The present metabolomic findings extend these observations by showing that caffeine treatment was accompanied by broad intracellular metabolic remodeling in LPS-stimulated RAW 264.7 macrophages. Rather than indicating a single dominant metabolic target, the curated me-

tabolite profile suggests coordinated changes across nucleotide-sugar metabolism, purine-related metabolism, amino acid/redox metabolism, central carbon metabolism, and lipid remodeling. One of the most prominent caffeine-associated changes was the increase in nucleotide-sugar intermediates, including UDP-N-acetylglucosamine, UDP-N-acetylgalactosamine, UDP-glucose, and GDP-mannose. These metabolites are central donors for glycosylation reactions and contribute to the biosynthesis and remodeling of glycoproteins, glycolipids, proteoglycans, and glycoconjugates (Varki, 2017; Viola, Munari, Sánchez-Rodríguez, Scolaro, & Castegna, 2019). In immune cells, glycosylation is closely associated with receptor function, cell–cell communication, inflammatory signaling, and membrane-associated immune responses (Li, Xie, Men, & Du, 2019; Varki, 2017; Viola et al., 2019). Therefore, the increased abundance of nucleotide-sugar metabolites in the LPS + caffeine group may indicate that caffeine treatment influenced glycosylation-related metabolic capacity and membrane-associated remodeling processes under LPS-stimulated conditions. This interpretation is also consistent with the pathway-level representation of amino sugar and nucleotide sugar metabolism in the curated metabolite set. One observation qualifies this interpretation. N-acetylneuraminic acid, the terminal sugar of sialylated glycans, was decreased rather than increased. CMP-N-acetylneuraminic acid, the immediate donor for sialylation, was not detected in this dataset. Therefore, we could not determine whether this change reflects increased consumption of sialic acid during glycan synthesis or reduced sialic acid availability.

Caffeine-associated alterations were also observed in nucleotide and purine-related metabolites. Caffeine is structurally related to purine metabolites and acts primarily as a non-selective antagonist of adenosine receptors (Daly, 2007; Fredholm et al., 1999; Jacobson et al., 2022). In the present study, changes in AICAR, inosinic acid, adenosine 3′,5′-diphosphate, nicotinamide ribotide, and cytidine suggest that caffeine treatment was associated with altered nucleotide turnover and purine-related metabolic remodeling in LPS-stimulated macrophages. Since purine metabolism is linked to energy balance, nucleotide biosynthesis, adenosine signaling, and immune cell activation, these changes may reflect a broader adjustment of nucleotide-associated metabolic pathways under inflammatory conditions (Daly, 2007; Fredholm et al., 1999; Haskó et al., 2008; Jacobson et al., 2022; Pasquini, Contri, Borea, Vincenzi, & Varani, 2021). Two of these changes are of particular interest. AICAR, an intermediate of de novo purine synthesis and a well-characterized activator of AMP-activated protein kinase, was decreased, whereas nicotinamide ribotide, an intermediate of the NAD+ salvage pathway, was increased; NAD+ salvage is closely tied to inflammatory macrophage function through NAMPT and CD38 activity (Cameron et al., 2019). Since neither AMPK activation nor NAD+ levels were measured, these are reported as directions requiring targeted follow-up rather than as evidence of altered energy sensing. However, because receptor activity, adenosine levels, and purine flux were not directly measured, these findings should be interpreted as metabolomic evidence of purine-related remodeling rather than direct evidence of adenosine receptor-mediated regulation.

Alterations in glutamine, glutamic acid, glutathione, and sulfur-containing intermediates also suggest that caffeine treatment affected amino acid- and redox-associated metabolism in LPS-stimulated RAW 264.7 macrophages. Glutamine and glutamate are central metabolic nodes that contribute to nitrogen metabolism, anaplerotic input into the tricarboxylic acid cycle, nucleotide biosynthesis, and antioxidant defense through glutathione production (Cruzat, Rogero, Keane, Curi, & Newsholme, 2018; Jha et al., 2015; Kelly & O'Neill, 2015; Lampropoulou et al., 2016; Mills et al., 2018; O'Neill et al., 2016; Ren et al., 2019; Tannahill et al., 2013). In inflammatory macrophages, glutamine/glutamate metabolism is closely linked to bioenergetic adaptation, redox balance, and

inflammatory mediator production (Jha et al., 2015; Kelly & O'Neill, 2015; Lampropoulou et al., 2016; Mills et al., 2018; O'Neill et al., 2016; Tannahill et al., 2013). In the present study, glutamine decreased, whereas glutamic acid increased, a pattern compatible with altered glutamine utilization; glutathione and the cysteine catabolism intermediate 3-sulfinylpyruvic acid both decreased. The decrease in glutathione indicates that caffeine treatment did not increase intracellular reduced glutathione under these conditions. This decrease may reflect either increased consumption or reduced synthesis. Because macrophage redox status is governed by regulatory pathways such as Nrf2/HO-1 signaling and by reactive oxygen species acting as signaling intermediates rather than by glutathione abundance alone (Brüne et al., 2013; Canton et al., 2021; Kwon et al., 2019), this change cannot by itself be equated with a shift in oxidative stress. L-Tryptophan decreased, while 5-hydroxy-L-tryptophan increased. In activated macrophages, tryptophan is catabolized predominantly through the indoleamine 2,3-dioxygenase/kynurenine route, which is central to immunometabolic regulation; no kynurenine pathway metabolites were detected in the present dataset, so this branch could not be evaluated. The annotation of 5-hydroxy-L-tryptophan, a serotonin pathway intermediate not typically prominent in macrophages, should also be regarded as putative pending MS/MS confirmation. However, because oxidative stress markers and glutathione redox ratios were not directly measured, these findings should be interpreted as metabolomic evidence of redox-associated remodeling rather than direct evidence of altered oxidative stress.

Caffeine-associated alterations were also observed in metabolites related to central carbon metabolism, including malic acid, citric acid, cis-2-methylaconitate, mesaconic acid, glycerol 3-phosphate, and glucose-related metabolites. LPS-stimulated macrophage activation is commonly associated with remodeling of glycolysis and mitochondrial metabolism, including changes in tricarboxylic acid cycle intermediates and related organic acids (Jha et al., 2015; Kelly & O'Neill, 2015; Lampropoulou et al., 2016; Mills et al., 2018; O'Neill et al., 2016; Tannahill et al., 2013). In the present study, the representation of glyoxylate and dicarboxylate metabolism, the citrate cycle, and related organic acid pathways suggests that caffeine treatment was associated with changes in central carbon metabolism under inflammatory conditions. These alterations may reflect adjustments in mitochondrial-associated metabolism, anaplerotic balance, or glycolysis-linked metabolic demand. Intracellular D-glucose decreased, and gluconic acid increased. A fall in intracellular glucose may reflect either increased consumption or reduced uptake, and the two cannot be distinguished without parallel measurement of extracellular glucose and lactate. Nevertheless, because isotope tracing, oxygen consumption, extracellular acidification, and targeted quantification of TCA intermediates were not performed, these data should be interpreted as evidence of central carbon metabolic remodeling rather than direct evidence of altered mitochondrial respiration or glycolytic flux.

One aspect of these central carbon metabolite changes deserves specific comment. The feature annotated as mesaconic acid, which decreased in the LPS + caffeine group, corresponds to a structural isomer of itaconate, a metabolite generated from cis-aconitate by aconitate decarboxylase 1 in LPS-activated macrophages and one of the principal endogenous regulators of inflammatory macrophage activation (Lampropoulou et al., 2016; Mills et al., 2018). Because itaconate, mesaconate, and citraconate share the same molecular formula and accurate mass, and because data-dependent MS/MS acquisition was not performed, these isomers were not resolved in the present dataset, and the annotation should be regarded as putative. The direction of the change is nevertheless notable: a decrease in this feature together with the observed increase in citric acid would be compatible with reduced diversion of citrate into the itaconate branch of the tricarboxylic acid cycle. This possibility warrants targeted, MS/MS-confirmed quantification,

because a caffeine-associated reduction in itaconate would carry different immunological implications from a straightforward anti-inflammatory effect, given that itaconate acts to restrain inflammatory macrophage activation. The decrease in cis-2-methylaconitate is more difficult to interpret, since this intermediate belongs to the methylcitrate cycle, which is not a canonical mammalian pathway, and its annotation likewise requires confirmation.

Lipid-related alterations represented another important component of caffeine-associated metabolic modulation. In the present study, LysoPC(18:1/0:0), LysoPC(O-18:0/0:0), PS(16:0/16:0), and phytosphingosine were decreased in the LPS + caffeine group, whereas PA(16:0/16:0), myristic acid, oleic acid, and 3-dehydrosphinganine were increased. These changes suggest that caffeine treatment was associated with selective remodeling of membrane-associated and signaling lipid metabolism under LPS-stimulated conditions. 3-Hydroxy-N^6,N^6,N^6-trimethyl-L-lysine, an intermediate of carnitine biosynthesis, showed one of the largest decreases in the curated set; together with the decrease in glycerol 3-phosphate and the increases in free myristic and oleic acid, this may indicate altered handling of fatty acids, although carnitine and acylcarnitines were not measured. The increase in 3-dehydrosphinganine, the first intermediate of de novo sphingolipid synthesis, alongside the decrease in phytosphingosine is compatible with altered flux through this pathway; however, phytosphingosine is a minor sphingoid base in mammalian cells, and a serum-derived contribution cannot be excluded.

Phospholipids are structural components of cellular membranes and also serve as precursors or modulators of bioactive lipid signaling pathways involved in innate immune responses (O'Donnell, Rossjohn, & Wakelam, 2018). In macrophages, glycerophospholipid metabolism, lysophospholipid turnover, fatty acid metabolism, and sphingolipid-associated signaling are closely linked to inflammatory activation and macrophage functional states (Huang, Schäfer-Elinder, Wu, Claesson, & Frostegård, 1999; O'Donnell et al., 2018; Qin, Qiu, & Zhao, 2014; Zhang et al., 2017). Therefore, the observed changes in lysophospholipids, phosphatidylserine, phosphatidic acid, fatty acids, and sphingolipid-related metabolites may reflect caffeine-associated remodeling of membrane composition and lipid signaling networks in LPS-stimulated RAW 264.7 macrophages.

The decrease in lysophosphatidylcholine-related metabolites may be particularly relevant, as lysophosphatidylcholine has been associated with pro-inflammatory macrophage activation and inflammatory mediator production (Huang et al., 1999; Qin et al., 2014). In contrast, the increase in PA(16:0/16:0) should be interpreted cautiously, because phosphatidic acid is a multifunctional lipid intermediate involved in membrane dynamics, phospholipid biosynthesis, and intracellular signaling (Lim et al., 2003; O'Donnell et al., 2018). Taken together, these lipid-related findings suggest that caffeine treatment did not globally suppress lipid metabolism but was associated with selective remodeling of membrane-associated and signaling lipid pathways during LPS-stimulated macrophage activation.

Pathway-level analysis provided additional biological context for the curated metabolite-level findings. Several pathways, including glyoxylate and dicarboxylate metabolism, glycerophospholipid metabolism, nitrogen metabolism, amino sugar and nucleotide sugar metabolism, alanine/aspartate/glutamate metabolism, arginine biosynthesis, and glycerolipid metabolism, showed raw p-values < 0.05. However, none remained statistically significant after FDR correction. Therefore, we interpreted these pathway-level findings as exploratory patterns of metabolite representation rather than statistically confirmed pathway enrichment. Two of these results require qualification. The highest-ranked pathway, glyoxylate and dicarboxylate metabolism, is populated in the KEGG database largely by tricarboxylic acid cycle intermediates such as citrate and malate; because the glyoxylate

cycle itself is not operative in mammalian cells, this ranking reflects the overlap of those metabolites with the pathway definition rather than glyoxylate cycle activity. Nitrogen metabolism, although showing a raw p-value < 0.05, was assigned a topological impact of zero, indicating that the matched metabolites occupy peripheral positions in the pathway and contribute little to its network structure. These pathway-level patterns were consistent with the curated metabolite-level findings, including alterations in UDP-sugar intermediates, glutamine/glutamate-related metabolites, organic acids, glutathione, lysophospholipids, phosphatidic acid, fatty acids, and sphingolipid-related metabolites. Importantly, these results should be interpreted as pathway-level representation of altered metabolite sets rather than direct evidence of pathway activation or inhibition.

In addition to the interpretation of the metabolomic data, it was of interest whether caffeine might interact directly with the receptor complex that initiates LPS signaling. The molecular docking analysis provided a complementary computational perspective on the possible interaction between caffeine and the TLR4/MD-2 ligand-recognition region. The most noteworthy finding of the present docking study is that caffeine preserved interactions with three of the four amino acid residues previously identified as critical for ligand recognition within the TLR4/MD-2 complex. Previous structural and molecular docking studies have consistently highlighted Thr319, Arg262, Lys362, and Tyr292 as key residues governing ligand recognition and stabilization, particularly for small-molecule TLR4/MD-2 inhibitors (Zhou et al., 2021). Although caffeine did not directly interact with Arg262, the preservation of contacts with Thr319, Lys362, and Tyr292 indicates that the xanthine scaffold adopts a binding orientation closely resembling those reported for previously described TLR4/MD-2 ligands. Among these residues, Lys362 and Tyr292 have been recognized as major contributors to ligand stabilization within the receptor interface. Accordingly, the predicted hydrogen-bonding interaction with Lys362 together with the π–π interaction involving Tyr292 supports the plausibility of the computationally predicted pose. However, these interactions are docking-derived predictions and do not establish experimental binding or dynamic stability of caffeine within the TLR4/MD-2 complex.

Another interesting observation is that caffeine adopted a binding mode distinct from that of lipid-based TLR4 antagonists such as Eritoran. Instead of deeply occupying the large hydrophobic cavity of MD-2, caffeine was positioned closer to the TLR4–MD-2 recognition interface while maintaining interactions with residues known to participate in ligand recognition. This surface-oriented binding mode is structurally plausible given the small molecular size, rigid xanthine scaffold, and polar character of caffeine. However, the docking analysis does not establish that caffeine perturbs LPS recognition or inhibits TLR4/MD-2 signaling. Overall, the docking results suggest a plausible interaction near the TLR4/MD-2 ligand-recognition region that warrants experimental validation. This study has several limitations. First, the untargeted LC–MS approach used in this study provides relative metabolite abundance data and does not directly measure metabolic flux or absolute metabolite concentrations. No internal standard was used in the untargeted metabolomics workflow; therefore, variability from extraction efficiency, sample injection, and instrumental response could not be corrected on an internal-standard basis. Analytical variability was instead controlled through pooled QC monitoring, QC-RSD filtering, blank filtering, technical replicate averaging, and total peak area normalization. Second, although metabolite annotation was supported by an in-house LC–MS library and complementary public databases, data-dependent MS/MS confirmation was not performed for all annotated features; therefore, putative annotations were interpreted cautiously. Third, the present study focused on intracellular metabolites, and extracellular metabolic exchange, cytokine release, nitric oxide production, and protein-level inflammatory signaling markers

were not assessed in parallel. Finally, the molecular docking analysis was exploratory and does not provide experimental evidence of caffeine binding to or inhibition of the TLR4/MD-2 complex. In addition, the metabolomic experiment compared LPS-stimulated cells with and without caffeine and did not include an unstimulated control group or a caffeine-only group; it is therefore not possible to determine which of the curated metabolite changes are specific to the inflammatory state, or to separate caffeine-associated effects from a possible interaction between caffeine and LPS stimulation. The results therefore indicate caffeine-associated metabolic differences under LPS-stimulated conditions rather than as reversal of LPS-induced metabolic reprogramming. Metabolite profiles were also obtained at a single time point (24 h) and at a single caffeine concentration; profiling was performed in negative ionization mode only, which limits coverage of metabolites that ionize preferentially in positive mode, and the data matrix was normalized to the total peak area of each sample rather than to cell number or protein content. Future studies using targeted metabolomics, isotope tracing, inflammatory mediator assays, and receptor-level validation experiments are required to clarify the mechanistic basis of caffeine-associated metabolic modulation in LPS-stimulated macrophages.

CONCLUSION

Overall, the present study shows that caffeine treatment was associated with a distinct intracellular metabolomic profile in LPS-stimulated RAW 264.7 macrophages. The curated metabolite set indicated coordinated alterations in nucleotide-sugar metabolism, purine-related metabolism, glutamine/glutamate-associated amino acid metabolism, redox-associated metabolism, central carbon metabolism, and lipid remodeling. These findings suggest that caffeine may influence the metabolic state of LPS-stimulated macrophages through broad metabolic modulation rather than through a single isolated metabolic pathway. Together, the metabolomic and exploratory docking results provide a framework for future targeted and functional studies investigating the role of caffeine in macrophage inflammatory metabolism.

AUTHOR CONTRIBUTION STATEMENT

OK: conceptualization, methodology, investigation, formal analysis, writing – original draft. AA: molecular docking analysis, investigation, visualization, writing – review and editing. VMK: conceptualization, supervision, validation, writing – review and editing. All authors have read and approved the submitted version of the manuscript.

CONFLICT OF INTEREST

The authors declare that there is no conflict of interest.

REFERENCES

Akira, S., & Takeda, K. (2004). Toll-like receptor signalling. *Nature Reviews Immunology, 4*(7), 499–511. doi:10.1038/nri1391

Arroyo-Xochihua, O., Zepeda, R. C., & Sánchez-Medina, A. (2026). RAW 264.7 macrophage cell line as a metabolomic model for analyzing and understanding inflammation processes. *Naunyn-Schmiedeberg's Archives of Pharmacology, 399*(7), 9527–9549. doi:10.1007/s00210-026-05038-w

Brüne, B., Dehne, N., Grossmann, N., Jung, M., Namgaladze, D., Schmid, T., . . . Weigert, A. (2013). Redox control of inflammation in macrophages. *Antioxidants & Redox Signaling, 19*(6), 595–637. doi:10.1089/ars.2012.4785

Cameron, A. M., Castoldi, A., Sanin, D. E., Flachsmann, L. J., Field, C. S., Puleston, D. J., . . . Pearce, E. J. (2019). Inflammatory macrophage dependence on NAD+ salvage is a consequence of reactive oxygen species–mediated DNA damage. *Nature Immunology, 20*(4), 420–432. doi:10.1038/s41590-019-0336-y

Canton, M., Sánchez-Rodríguez, R., Spera, I., Venegas, F. C., Favia, M., Viola, A., & Castegna, A. (2021). Reactive oxygen species in macrophages: Sources and targets. *Frontiers in Immunology, 12*, 734229. doi:10.3389/fimmu.2021.734229

Cruzat, V., Rogero, M. M., Keane, K. N., Curi, R., & Newsholme, P. (2018). Glutamine: Metabolism and immune function, supplementation and clinical translation. *Nutrients, 10*(11), 1564. doi:10.3390/nu10111564

Čuperlović-Culf, M., Barnett, D. A., Culf, A. S., & Chute, I. (2010). Cell culture metabolomics: Applications and future directions. *Drug Discovery Today, 15*(15–16), 610–621. doi:10.1016/j.drudis.2010.06.012

Daly, J. W. (2007). Caffeine analogs: Biomedical impact. *Cellular and Molecular Life Sciences, 64*(16), 2153–2169. doi:10.1007/s00018-007-7051-9

Doğan, Z., Kutluay, V. M., Genç, Y., & Saraçoğlu, İ. (2023). Interactions between phenolic constituents of *Scutellaria salviifolia* and key targets associated with inflammation: Network pharmacology, molecular docking analysis and in vitro assays. *Journal of Biomolecular Structure and Dynamics, 41*(4), 1281–1294. doi:10.1080/07391102.2021.2019119

Domenick, T. M., Gill, E. L., Vedam-Mai, V., & Yost, R. A. (2021). Mass spectrometry-based cellular metabolomics: Current approaches, applications, and future directions. *Analytical Chemistry, 93*(1), 546–566. doi:10.1021/acs.analchem.0c04363

Dunn, W. B., Bailey, N. J. C., & Johnson, H. E. (2005). Measuring the metabolome: Current analytical technologies. *Analyst, 130*(5), 606–625. doi:10.1039/B418288J

Fiehn, O. (2002). Metabolomics—the link between genotypes and phenotypes. *Plant Molecular Biology, 48*(1–2), 155–171. doi:10.1023/A:1013713905833

Fredholm, B. B., Bättig, K., Holmén, J., Nehlig, A., & Zvartau, E. E. (1999). Actions of caffeine in the brain with special reference to factors that contribute to its widespread use. *Pharmacological Reviews, 51*(1), 83–133. doi:10.1016/S0031-6997(24)01396-6

Friesner, R. A., Banks, J. L., Murphy, R. B., Halgren, T. A., Klicic, J. J., Mainz, D. T., . . . Shenkin, P. S. (2004). Glide: A new approach for rapid, accurate docking and scoring. 1. Method and assessment of docking accuracy. *Journal of Medicinal Chemistry, 47*(7), 1739–1749. doi:10.1021/jm0306430

Gusev, E., & Zhuravleva, Y. (2022). Inflammation: A new look at an old problem. *International Journal of Molecular Sciences, 23*(9), 4596. doi:10.3390/ijms23094596

Haskó, G., Linden, J., Cronstein, B., & Pacher, P. (2008). Adenosine receptors: Therapeutic aspects for inflammatory and immune diseases. *Nature Reviews Drug Discovery, 7*(9), 759–770. doi:10.1038/nrd2638

Huang, Y.-H., Schäfer-Elinder, L., Wu, R., Claesson, H.-E., & Frostegård, J. (1999). Lysophosphatidylcholine (LPC) induces proinflammatory cytokines by a platelet-activating factor (PAF) receptor-dependent mechanism. *Clinical and Experimental Immunology, 116*(2), 326–331. doi:10.1046/j.1365-2249.1999.00871.x

Hwang, J.-H., Kim, K.-J., Ryu, S.-J., & Lee, B.-Y. (2016). Caffeine prevents LPS-induced inflammatory responses in RAW264.7 cells and zebrafish. *Chemico-Biological Interactions, 248*, 1–7. doi:10.1016/j.cbi.2016.01.020

Jacobson, K. A., Gao, Z.-G., Matricon, P., Eddy, M. T., & Carlsson, J. (2022). Adenosine A2A receptor antagonists: From caffeine to selective non-xanthines. *British Journal of Pharmacology, 179*(14), 3496–3511. doi:10.1111/bph.15103

Jha, A. K., Huang, S. C.-C., Sergushichev, A., Lampropoulou, V., Ivanova, Y., Loginicheva, E., . . . Artyomov, M. N. (2015). Network integration of parallel metabolic and transcriptional data reveals metabolic modules that regulate macrophage polarization. *Immunity, 42*(3), 419–430. doi:10.1016/j.immuni.2015.02.005

Kelly, B., & O'Neill, L. A. J. (2015). Metabolic reprogramming in macrophages and dendritic cells in innate immunity. *Cell Research, 25*(7), 771–784. doi:10.1038/cr.2015.68

Kovács, E. G., Alatshan, A., Budai, M. M., Czimmerer, Z., Bíró, E., & Benkő, S. (2021). Caffeine has different immunomodulatory effect on the cytokine expression and NLRP3 inflammasome function in various human macrophage subpopulations. *Nutrients, 13*(7), 2409. doi:10.3390/nu13072409

Kwon, D. H., Cha, H.-J., Lee, H., Hong, S.-H., Park, C., Park, S.-H., . . . Choi, Y. H. (2019). Protective effect of glutathione against oxidative stress-induced cytotoxicity in RAW 264.7 macrophages through activating the nuclear factor erythroid 2-related factor-2/heme oxygenase-1 pathway. *Antioxidants, 8*(4), 82. doi:10.3390/antiox8040082

Lampropoulou, V., Sergushichev, A., Bambouskova, M., Nair, S., Vincent, E. E., Loginicheva, E., . . . Artyomov, M. N. (2016). Itaconate links inhibition of succinate dehydrogenase with macrophage metabolic remodeling and regulation of inflammation. *Cell Metabolism, 24*(1), 158–166. doi:10.1016/j.cmet.2016.06.004

Li, Y., Xie, M., Men, L., & Du, J. (2019). O-GlcNAcylation in immunity and inflammation: An intricate system (Review). *International Journal of Molecular Medicine, 44*(2), 363–374. doi:10.3892/ijmm.2019.4238

Lim, H.-K., Choi, Y.-A., Park, W., Lee, T., Ryu, S. H., Kim, S.-Y., . . . Baek, S.-H. (2003). Phosphatidic acid regulates systemic inflammatory responses by modulating the Akt–mammalian target of rapamycin–p70 S6 kinase 1 pathway. *Journal of Biological Chemistry, 278*(46), 45117–45127. doi:10.1074/jbc.M303789200

Lu, Y.-C., Yeh, W.-C., & Ohashi, P. S. (2008). LPS/TLR4 signal transduction pathway. *Cytokine, 42*(2), 145–151. doi:10.1016/j.cyto.2008.01.006

Meizlish, M. L., Franklin, R. A., Zhou, X., & Medzhitov, R. (2021). Tissue homeostasis and inflammation. *Annual Review of Immunology, 39*, 557–581. doi:10.1146/annurev-immunol-061020-053734

Mills, E. L., Ryan, D. G., Prag, H. A., Dikovskaya, D., Menon, D., Zaslona, Z., . . . O'Neill, L. A. J. (2018). Itaconate is an anti-inflammatory metabolite that activates Nrf2 via alkylation of KEAP1. *Nature, 556*(7699), 113–117. doi:10.1038/nature25986

Molteni, M., Gemma, S., & Rossetti, C. (2016). The role of Toll-like receptor 4 in infectious and noninfectious inflammation. *Mediators of Inflammation, 2016*, 6978936. doi:10.1155/2016/6978936

Nicholson, J. K., Lindon, J. C., & Holmes, E. (1999). "Metabonomics": Understanding the metabolic responses of living systems to pathophysiological stimuli via multivariate statistical analysis of biological NMR spectroscopic data. *Xenobiotica, 29*(11), 1181–1189. doi:10.1080/004982599238047

O'Donnell, V. B., Rossjohn, J., & Wakelam, M. J. O. (2018). Phospholipid signaling in innate immune cells. *Journal of Clinical Investigation, 128*(7), 2670–2679. doi:10.1172/JCI97944

O'Neill, L. A. J., Kishton, R. J., & Rathmell, J. (2016). A guide to immunometabolism for immunologists. *Nature Reviews Immunology, 16*(9), 553–565. doi:10.1038/nri.2016.70

Park, B. S., Song, D. H., Kim, H. M., Choi, B.-S., Lee, H., & Lee, J.-O. (2009). The structural basis of lipopolysaccharide recognition by the TLR4–MD-2 complex. *Nature, 458*(7242), 1191–1195. doi:10.1038/nature07830

Pasquini, S., Contri, C., Borea, P. A., Vincenzi, F., & Varani, K. (2021). Adenosine and inflammation: Here, there and everywhere. *International Journal of Molecular Sciences, 22*(14), 7685. doi:10.3390/ijms22147685

Patti, G. J., Yanes, O., & Siuzdak, G. (2012). Metabolomics: The apogee of the omics trilogy. *Nature Reviews Molecular Cell Biology, 13*(4), 263–269. doi:10.1038/nrm3314

Qin, X., Qiu, C., & Zhao, L. (2014). Lysophosphatidylcholine perpetuates macrophage polarization toward classically activated phenotype in inflammation. *Cellular Immunology, 289*(1–2), 185–190. doi:10.1016/j.cellimm.2014.04.010

Ren, W., Xia, Y., Chen, S., Wu, G., Bazer, F. W., Zhou, B., . . . Yin, Y. (2019). Glutamine metabolism in macrophages: A novel target for obesity/type 2 diabetes. *Advances in Nutrition, 10*(2), 321–330. doi:10.1093/advances/nmy084

Schrödinger, LLC. (2019). *LigPrep* (Schrödinger Release 2019-4) [Computer software]. New York, NY: Author.

Schrödinger, LLC. (2023). *Maestro* (Schrödinger Release 2023-4) [Computer software]. New York, NY: Author.

Taciak, B., Białasek, M., Braniewska, A., Sas, Z., Sawicka, P., Kiraga, Ł., . . . Król, M. (2018). Evaluation of phenotypic and functional stability of RAW 264.7 cell line through serial passages. *PLoS ONE, 13*(6), e0198943. doi:10.1371/journal.pone.0198943

Tannahill, G. M., Curtis, A. M., Adamik, J., Palsson-McDermott, E. M., McGettrick, A. F., Goel, G., . . . O'Neill, L. A. J. (2013). Succinate is an inflammatory signal that induces IL-1β through HIF-1α. *Nature, 496*(7444), 238–242. doi:10.1038/nature11986

Varki, A. (2017). Biological roles of glycans. *Glycobiology, 27*(1), 3–49. doi:10.1093/glycob/cww086

Viola, A., Munari, F., Sánchez-Rodríguez, R., Scolaro, T., & Castegna, A. (2019). The metabolic signature of macrophage responses. *Frontiers in Immunology, 10*, 1462. doi:10.3389/fimmu.2019.01462

Zhang, A., Sun, H., Xu, H., Qiu, S., & Wang, X. (2013). Cell metabolomics. *OMICS: A Journal of Integrative Biology, 17*(10), 495–501. doi:10.1089/omi.2012.0090

Zhang, C., Wang, Y., Wang, F., Wang, Z., Lu, Y., Xu, Y., . . . Yu, H. (2017). Quantitative profiling of glycerophospholipids during mouse and human macrophage differentiation using targeted mass spectrometry. *Scientific Reports, 7*(1), 412. doi:10.1038/s41598-017-00341-2

Zhou, S., Zou, H., Huang, G., Chen, G., Zhou, X., & Huang, S. (2021). Design, synthesis and anti-rheumatoid arthritis evaluation of double-ring conjugated enones. *Bioorganic Chemistry, 109*, 104701. doi:10.1016/j.bioorg.2021.104701